STUDIA UNIVERSITATIS BABES-BOLYAI, CHEMIA, LIV, 1, 2009

Dedicated to Professor Liviu Literat, at his 80th anniversary

SIMULATION OF A POLYMERIZATION LAMINAR FLOW REACTOR

IONUȚ BANU[ab], SORIN BÎLDEA[a], GRIGORE BOZGA[a], JEAN-PIERRE PUAUX[b]

ABSTRACT. The paper presents a simulation study of the methyl methacrylate solution polymerization process occurring in a laminar flow tubular reactor. The simulation results are evidencing the main particularities of the polymerization process induced by the laminar flow of the reaction mixture, as well as the practical suitability of this operating regime. The influence of the main process parameters on the reactor behavior is investigated. Also a comparison of the process simulation results obtained in laminar flow and plug flow assumptions is presented.

Keywords: *MMA polymerization, laminar flow reactor*

INTRODUCTION

The poly-methyl methacrylate (PMMA) is a polymer with good optical and mechanical properties. Currently it is obtained by free-radical polymerization of the methyl methacrylate (MMA), which can be performed in batch or tubular reactors. Solution polymerization is a convenient technique to avoid the usual heat transfer difficulties specific for bulk polymerization. The usual solvents for polymerization of MMA are toluene [1, 2] and ethyl acetate [3, 4], while azobis-isobutyronitrile (AIBN) or benzoyl peroxide (BPO) are used as initiators. One of the difficulties in modeling MMA polymerization system is the description of diffusion phenomenon in viscous reaction mixture (the so-called gel effect or Trommsdorf effect) [5]. For bulk polymerization, the gel effect is important at high monomer conversions. For solution polymerization, it is significant at high monomer to solvent ratios. A complete study of the behavior of a MMA semi-batch polymerization reactor with solvent and monomer addition in different operating conditions was published by Louie and Soong [6].

[a] *Universitatea Politehnica din Bucureşti, Facultatea de Chimie Aplicată şi Ştiința Materialelor, Str. Polizu, Nr. 1, RO-011061 Bucureşti, Romania, g_bozga@chim.upb.ro*
[b] *Université de Lyon, Université Claude Bernard, Lyon, France*

The description of the mixture flow is one of the most important issues in the building of a mathematical model for the polymerization processes taking place in tubular reactors. Ideal flow models were used by Baillgou et Soong [7], Ponnuswamy et al [1] and Crowley et Choi [8]. They considered constant axial flow velocities with small corrections due to the density change [7, 9]. The complexity of the kinetic mechanism and the heat transfer which is hindered by the varying viscosity also make difficult the development of the mass and heat balance equations.

It is well known that, on axial direction of a tubular reactor, the convective transport is dominant, while in the radial direction the transport by diffusion mechanism is more important. The validity of these hypotheses was verified in the published literature [10, 11]. Cintron-Cordero et al [12] developed a two-dimensional flow model and compared the flow equations with or without the convective terms in radial direction. They observed that the errors are smaller than 3 % when the radial convection was neglected. Lynn et al [13] showed that the hypothesis of constant axial velocity will generate some errors due to the large variations in viscosity of the reaction mixture. They also proposed a method to calculate the profile of the axial velocity in a two-dimensional model, which was implemented in other published studies (Wyman et Carter [14], Baillagou et Soong [2]). If the axial dispersion is taken into account, the solution is obtained by discretization of both axial and radial directions [9, 11]. If axial dispersion is not considered, the method of lines is commonly used for the discretization in radial direction [15].

The objective of this study is to theoretically investigate the main features of the MMA solution polymerization process in a laminar flow tubular reactor. The kinetic model for the MMA solution polymerization process was chosen in one of our previous papers [16] by reviewing the published kinetic models. Further it is used to solve the mathematical model of MMA laminar flow polymerization reactor. The mathematical model and the solution method are discussed. Afterwards, the results of the simulation study as well as the influence of various operating parameters on the reactor behavior are presented and analyzed.

RESULTS AND DISCUSSIONS

Mathematical model of the MMA polymerization process in a laminar flow tubular reactor

The polymerization technique investigated in this work is the steady state MMA polymerization in solution. The kinetic model published by Baillagou and Soong [7, 17] is used. The gel effect is described by the model proposed by Chiu et al [5], the constitutive equations being presented in Table 1. The characteristics of the reactor are displayed in

Table 2. Because of the strong exothermicity of the polymerization reaction, a high value of length to diameter ratio is chosen, which provides a sufficiently high heat transfer area.

Table 1. Gel effect constitutive equations [17]

$$k_t = \frac{k_{t,0}}{1+\frac{k_{t,0}\theta_t\lambda_0}{D_{ef}}};\ k_p = \frac{k_{p,0}}{1+\frac{k_{p,0}\theta_p\lambda_0}{D_{ef}}};\ D_{ef} = \exp\left(\frac{2.3\phi_m}{A+B\phi_m}\right)$$

$$\theta_t = \frac{1}{4.4533\times10^{18} c_{I,0} \exp\left(-\frac{17413}{T}\right)}$$

$$\theta_p = \frac{1}{2.5292\times10^{15} \exp\left(-\frac{14092}{T}\right)}$$

$$A = 0.168 - 8.21\times10^{-6}\left(T - T_{gp}\right)^2;\ \text{B} = 0.03$$

Table 2. Reactor characteristics

Process parameter	Numerical value
Total mass flow rate / [kg/s]	10^{-3}
Feed initiator concentration (c_{I0}) / [mole/L]	0.05
Toluene mass fraction in the feed	0.5
Reactor length / [m]	8
Reactor diameter (d_t) / [m]	2×10^{-2}
Feed temperature / [^{O}C]	80
Thermal agent temperature / [^{O}C]	80

The radial convection terms are ignored because the tube length is much larger than the radius. In the axial direction, mass diffusion and heat conduction are assumed to be negligible compared to the convective terms. Variations of monomer conversion and consequently of mixture viscosity and density produce strong variations in the axial velocities. The flow is considered fully developed at the reactor entrance and the velocity profiles along the reactor axis are calculated using the method proposed by Lynn and Huff [13]. The physical properties (density, viscosity, thermal conductivity) of the reaction mixture are estimated using relations published in literature [2, 7, 17, 18].

The mathematical model of the polymerization process includes the mass balance equations for initiator (1) and monomer (2), the equations describing the evolutions of the *m*-moments (*m*=0, 1, 2) of live and dead polymer molecular weight distribution (3) and (4), as well as heat balance equation (5).

$$\frac{\partial c_I}{\partial z} = -\frac{c_I}{u_z}\frac{\partial u_z}{\partial z} + \frac{1}{u_z}\left(\frac{D}{r}\frac{\partial c_I}{\partial r} + D\frac{\partial^2 c_I}{\partial r^2}\right) + \frac{r_I}{u_z} \tag{1}$$

$$\frac{\partial c_M}{\partial z} = -\frac{c_M}{u_z}\frac{\partial u_z}{\partial z} + \frac{1}{u_z}\left(\frac{D}{r}\frac{\partial c_M}{\partial r} + D\frac{\partial^2 c_M}{\partial r^2}\right) + \frac{r_M}{u_z} \tag{2}$$

$$\frac{\partial \lambda_m}{\partial z} = -\frac{\lambda_m}{u_z}\frac{\partial u_z}{\partial z} + \frac{1}{u_z}\left(\frac{D}{r}\frac{\partial \lambda_m}{\partial r} + D\frac{\partial^2 \lambda_m}{\partial r^2}\right) + \frac{r_{\lambda_m}}{u_z} \tag{3}$$

$$\frac{\partial \mu_m}{\partial z} = -\frac{\mu_m}{u_z}\frac{\partial u_z}{\partial z} + \frac{1}{u_z}\left(\frac{D}{r}\frac{\partial \mu_m}{\partial r} + D\frac{\partial^2 \mu_m}{\partial r^2}\right) + \frac{r_{\mu_m}}{u_z} \tag{4}$$

$$\frac{\partial T}{\partial z} = \frac{1}{\rho c_p u_z}\left(\frac{k}{r}\frac{\partial T}{\partial r} + k\frac{\partial^2 T}{\partial r^2}\right) + \frac{r_T}{\rho c_p u_z} \tag{5}$$

Axial symmetry, the absence of the mass transfer through the reactor wall and the continuity of heat flux at the reactor wall impose the following boundary conditions:

$$\begin{aligned} r = 0:\ & \frac{\partial c_M}{\partial r} = \frac{\partial c_I}{\partial r} = \frac{\partial \lambda_m}{\partial r} = \frac{\partial \mu_m}{\partial r} = \frac{\partial T}{\partial r} = 0 \\ r = R:\ & \frac{\partial c_M}{\partial r} = \frac{\partial c_I}{\partial r} = \frac{\partial \lambda_m}{\partial r} = \frac{\partial \mu_m}{\partial r} = 0,\ \frac{\partial T}{\partial r} = \frac{U}{k}\left(T_b - T\right) \end{aligned} \tag{6}$$

The inlet boundary conditions are:

$$z = 0: c_M = c_{M0}\ ,\ c_I = c_{I0}\ ,\ \lambda_m = 0\ ,\ \mu_m = 0\ ,\ T = T_f \tag{7}$$

It is considered that the main resistance to the heat transfer occurs inside the reactor. Therefore, the overall heat transfer coefficient, U, is approximated by the internal partial heat transfer coefficient calculated by the equation (8), where the variation of the viscosity at the wall is neglected and the ratio η / η_p approaches unity [18]:

$$Nu\left(\frac{\alpha d_t}{k}\right) = 3.66 + \frac{0.19Gz^{0.8}}{1+0.177Gz^{0.467}}\left(\frac{\eta}{\eta_p}\right)^{0.14} \tag{8}$$

The generating terms r_p (with p = I, M, λ_m, μ_m, T) in equations (1) - (5) are [1]:

$$r_I = -k_d c_I \tag{9}$$

$$r_M = -\left(k_p + k_{tm}\right) c_M \lambda_0 \tag{10}$$

$$r_{\lambda_0} = 2 f k_d c_I - k_t \lambda_0^2 \tag{11}$$

$$r_{\lambda_1} = 2 f k_d c_I + k_p c_M \lambda_0 + \left(k_{tm} c_M + k_{ts} c_S\right)\left(\lambda_0 - \lambda_1\right) - k_t \lambda_0 \lambda_1 \tag{12}$$

$$r_{\lambda_2} = 2 f k_d c_I + \left(2\lambda_1 + \lambda_0\right) k_p c_M + \left(k_{tm} c_M + k_{ts} c_S\right)\left(\lambda_0 - \lambda_2\right) - k_t \lambda_0 \lambda_2 \tag{13}$$

$$r_{\mu_0} = \left(k_{tm} c_M + k_{ts} c_S\right) \lambda_0 + \left(k_{td} + 0.5 k_{tc}\right) \lambda_0^2 \tag{14}$$

$$r_{\mu_1} = \left(k_{tm} c_M + k_{ts} c_S\right) \lambda_1 + k_t \lambda_0 \lambda_1 \tag{15}$$

$$r_{\mu_2} = \left(k_{tm} c_M + k_{ts} c_S\right) \lambda_2 + k_t \lambda_0 \lambda_2 \tag{16}$$

In the energy balance, as generally accepted, only the heat generated in propagation reactions and chain transfer to monomer is considered [7, 17]:

$$r_T = -\Delta H_p \left(k_p + k_{tm}\right) c_M \lambda_0 \tag{17}$$

The polymerization enthalpy, $\Delta H_p = -5.48 \times 10^4 \, \mathrm{J/mol}$, is taken from the reference [19]. The same diffusivity coefficient having a value of $D = 10^{-10}$ m^2/s is used in equations (1) - (4) for all the species [2].

In this work the derivatives with respect to the radial direction are approximated by a second order finite difference scheme. After discretization, the equation (1) becomes:

$$\frac{dc_{M,i}}{dz} = c_{M,i+1}\frac{1}{u_{z,i}}A_i + c_{M,i}\frac{1}{u_{z,i}}\left(-\frac{\partial u_{z,i}}{\partial z} - B_i\right) + c_{M,i-1}\frac{1}{u_{z,i}}C_i + \frac{r_{M,i}}{u_{z,i}} \quad (18)$$

Where the coefficients A_i, B_i, C_i are given by:

$$A_i = \frac{D}{2r_i\Delta r} + \frac{D}{(\Delta r)^2};\ B_i = -\frac{2D}{(\Delta r)^2};\ C_i = -\frac{D}{2r_i\Delta r} + \frac{D}{(\Delta r)^2},\ i = 2,3,..,N \quad (19)$$

At i =1 the equation (1) becomes indeterminate since both r and $\frac{\partial c_M}{\partial r}$ be-come zero. Applying the l'Hospital rule and assuming symmetry about the centerline [20]:

$$A_1 = \frac{4D}{(\Delta r)^2};\ B_1 = -\frac{4D}{(\Delta r)^2};\ C_1 = 0 \quad (20)$$

To minimize the calculation effort, the derivative $\frac{\partial u_z}{\partial z}$ was approximated by finite difference ratios:

$$\frac{\partial u_{z,k}}{\partial z} = \frac{u_{z,k} - u_{z,k-1}}{z_k - z_{k-1}} \quad (21)$$

where k refers to integration steps in the axial direction.

As a result, the original PDE's were transformed into a system of ODE's along the axial coordinate. The ODE's were solved by a Runge-Kutta procedure method implemented in MATLAB® [21].

Reactor simulation

In order to select the number of intervals on the radial coordinate, a comparison of different discretization grids was performed. Practically identical results were obtained when the number of grid points was increased over 50. Therefore, a number of 50 radial points was chosen, as a compromise between accuracy and calculation effort.

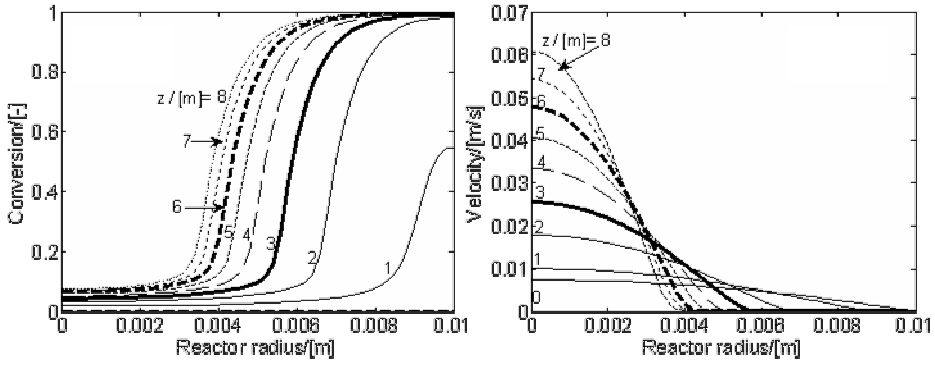

Figure 1. Profiles for monomer conversion (left) and axial velocity (right), at different positions (z) along the reactor.

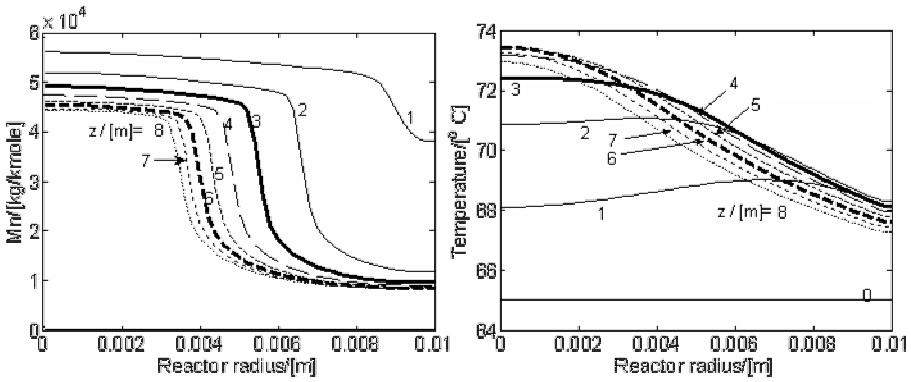

Figure 2. Number-average molecular weights (left) and temperature (right) profiles, at different positions (z) along the reactor.

Figures 1 and 2 present simulation results for the reactor with characteristics given in Table 2. The radial conversion profiles are relatively abrupt, with a fast transition from small values to almost complete conversion (Figure 1). As seen from Figure 1, two flowing zones are developed inside the tubular reactor: a central zone where the fluid velocity is relatively high and a peripheral (plugged) zone where the fluid velocity is relatively low, approaching zero in the proximity of the wall. Consequently, the maximum residence time occurs in the neighborhood of the wall, and minimum one in the center of tube. The differences in residence times give monomer conversions that drastically vary in radial direction, with values smaller than 10 % in the central zone and nearly 100% in the peripheral zone.

Figure 2 presents radial profiles of the number average molecular weights and temperature. In the plugged region close to the wall the polymer number-average molecular weight drastically decreases. This could be explained

by the small ratio of propagation to the termination rate, unfavorable to the formation of long chains, in the last two thirds of reactor length. Due to low amounts of monomer, the polymer radicals initiated in this region present a slow growth. Moreover, the high concentration of solvent promotes termination by chain transfer to solvent, finishing prematurely the newly produced chains.

Due to the high ratio of heat transfer area to reaction volume, only a moderate rise of the reaction temperature along the reactor is observed (Figure 2). The radial temperature profile presents a maximum, which moves from the neighborhood of the wall towards the center, as the axial position increases. This is explained by the heat generation rate, higher in the peripheral zone corresponding to the first meters of reactor length.

Influence of heat transfer area

To investigate the influence of the ratio between heat transfer area and reaction volume, the reactor diameter and length were varied keeping constant the mean residence time (defined as the ratio between the reactor volume and feed volumetric flow) of the reaction mixture through the polymerization reactor. The dimensions of the reactors used in these simulations are presented in Table 3, the other process parameters being specified in Table 2. In this section, only the results for extremes configurations are presented (Reactor 2 and Reactor 3), the others being already presented above.

Table 3. Reactor configurations

Reactor configuration	Length, [m]	Diameter, [m]
Reactor 1	8	2×10^{-2}
Reactor 2	2	4×10^{-2}
Reactor 3	32	1×10^{-2}

The results illustrated in Figures 3 to 5 prove that the reactor with high ratio of heat transfer area to reactor volume produces more homogenous final products and assures a more even thermal regime. The homogeneity is proved by the values of polydispersion index, a maximum value of 5 being obtained for Reactor 2 comparatively with a maximum value of 3 for Reactor 3.

As seen from Figure 5, the temperature profiles in Reactor 3 are more uniform due to a higher heat transfer area that is allowing a more efficient evacuation of the reaction heat. Moreover, the maximum value is located at the reactor centerline.

Comparatively, the temperature profiles in the Reactor 2 case present an evident maximum, shifted to the centerline only with advancement of the polymerization mixture along the axial coordinate of the reactor. A rise in temperature of almost 3 ℃ for Reactor 3 pr oduces higher molecular weight polymer close to the reactor wall, due to the small influence of chain transfer to solvent reaction in this region.

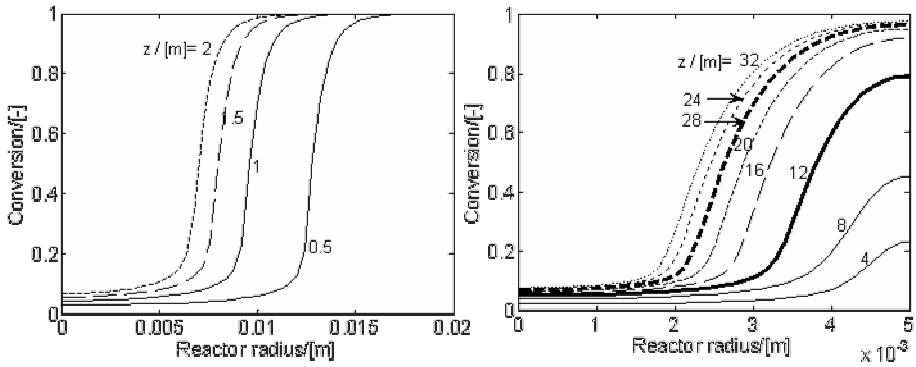

Figure 3. Radial profiles of monomer conversion, at different positions along the reactor. Left: Reactor 2; Right: Reactor 3.

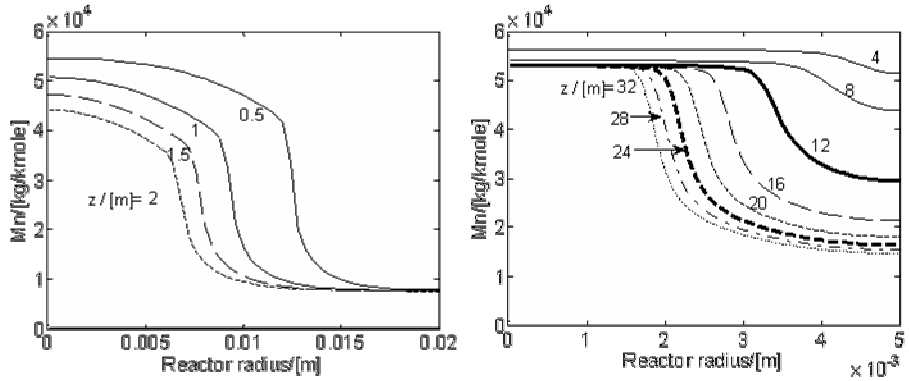

Figure 4. Radial profiles for number-average molecular weights, at different positions (z) along the reactor. Left: Reactor 2; Right: Reactor 3.

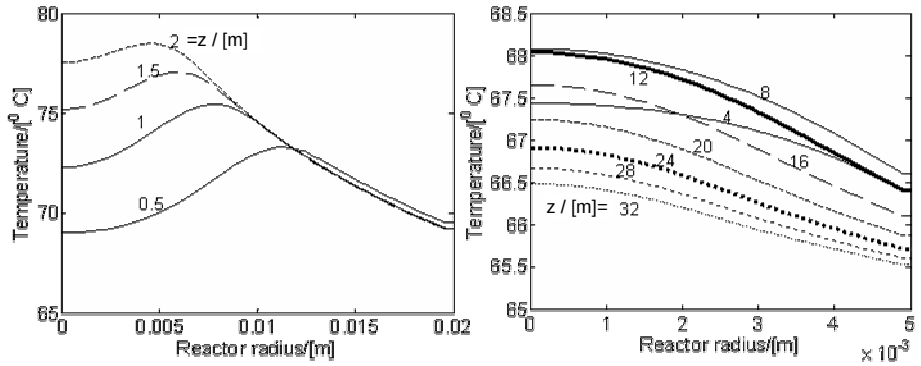

Figure 5. Radial profiles for temperature, at different positions (z) along the reactor. Left: Reactor 2; Right: Reactor 3.

Influence of initiator concentration

The initiator concentration has an important role in MMA polymerization, higher initiator concentrations producing polymers with lower molecular weights. Three values for the initiator concentrations (0.025, 0.05 and 0.1 mole/L) were tested for the Reactor 1 configuration (Table 3).

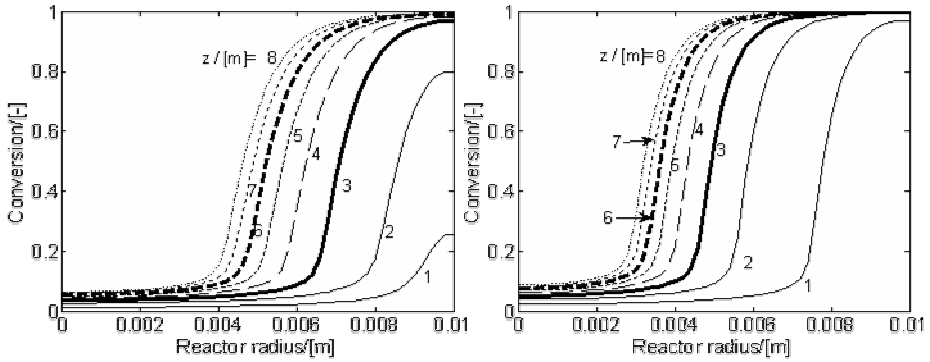

Figure 6. Monomer conversion profiles for initial initiator concentration of 0.025 mole/L (left) and 0.1 mole/L (right).

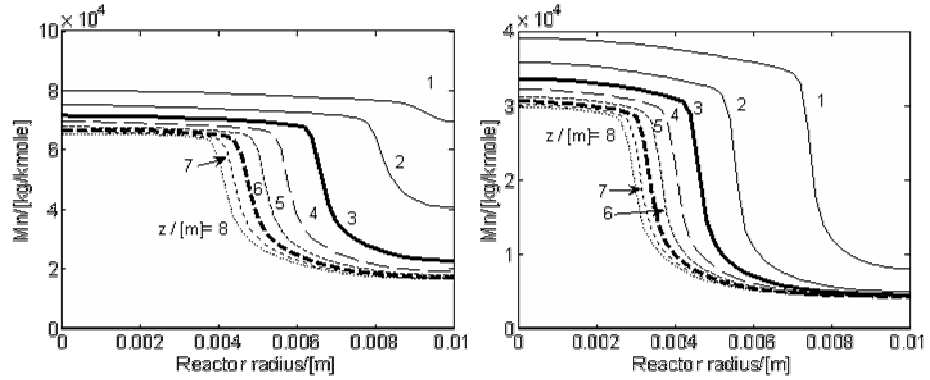

Figure 7. Number average molecular weight profiles for initial initiator concentration of 0.025 mole/L (left) and 0.1 mole/L (right).

Small initiator concentrations lead to a low initiation rate, and consequently to a small number of live polymer chains. This has two effects: first, a decrease of propagation rate having as result a low monomer conversion on the first 2 m of the reactor (Figure 6); second, an important increase of final polymer molecular weight (Figure 7). Also a small propagation rate decreases the amount of heat generated (low temperature levels) with an

increasing effect on the polymer molecular weight. Consequently, the initial initiator concentration proves to be an important parameter to control the final molecular weights of the polymer.

Influence of solvent concentration

It is well known that higher solvent fraction improves the heat transfer but also induces higher solvent separation costs. Three solvent mass fractions were tested for Reactor 1 configuration (Table 3).

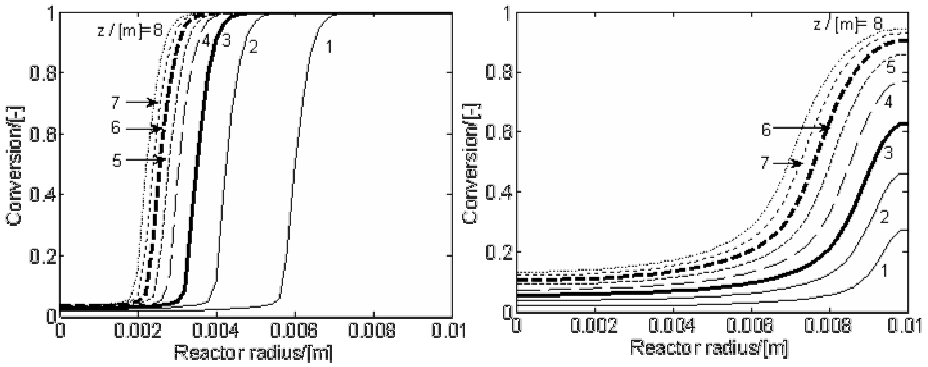

Figure 8. Monomer conversion profiles for smallest (ws = 0.3, left) and highest (ws = 0.7, right) feed weight solvent fraction.

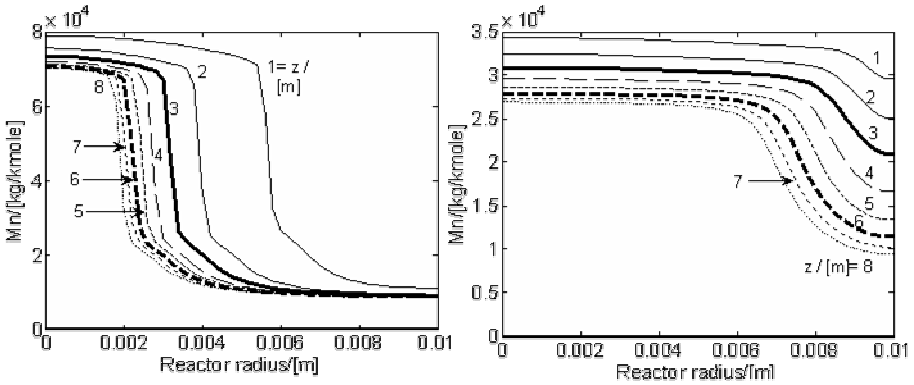

Figure 9. Number-average molecular weight for smallest (ws = 0.3, left) and highest (ws = 0.7, right) feed solvent fraction.

Increasing the fraction of solvent leads to lower reaction temperature through two mechanisms: a) less heat is generated due to lower amount of monomer; b) heat transfer through the wall is improved due to a lower resistance. Because the propagation step has a higher activation energy

compared to the termination reactions, the conversion is lower (Figure 8) and shorter chains are obtained (Figure 9). Smaller monomer concentration additionally contributes to lower propagation rates, with the same effect.

It should be remarked that increasing the solvent concentration leads to a polymer product with a more homogeneous molecular weight distribution. Thus, the polydispersion index is 7.65 and 2.27, for solvent fraction of 0.3 and 0.7, respectively.

The simulation results presented above are evidencing that the velocity profile of the laminar flow leads to a polymer of lower quality and the reactor volume is less efficiently used. This drawback becomes more important when the reaction mixture contains less solvent. The use of static mixers could change the velocity profile in order to approach the ideal case of plug-flow. This will be analyzed in the following section.

Comparison between laminar flow and plug flow reactor

A comparison between the simulation results obtained in the plug flow and laminar flow assumptions was finally performed (Figure 10). For the laminar flow polymerization tubular reactor, the values of monomer conversion and number-average molecular weight presented here are averages over the reactor cross-section.

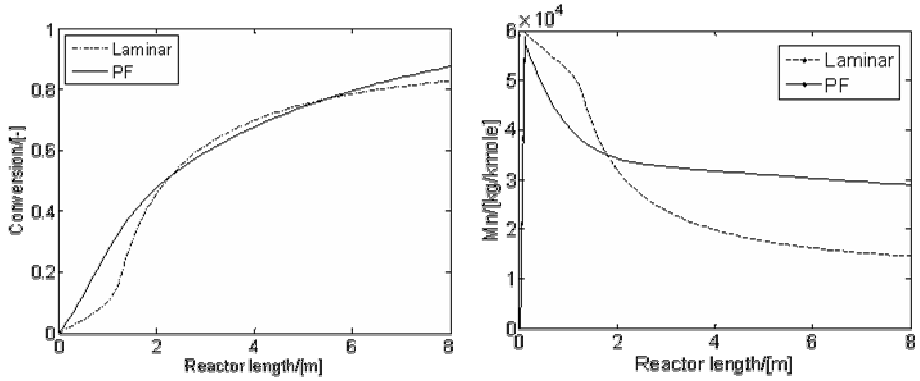

Figure 10. Plug flow and laminar flow reactor simulated monomer conversion and number-average molecular weights axial profiles (Reactor 1).

The two models predict similar values for the monomer conversion. However, the plug-flow reactor produces a polymer with a higher molecular weight and a narrow distribution (the polydispersion index of the final product is 2.13, compared to 3.21 for the laminar flow reactor). This is an argument for the practical effectiveness of static mixers in tubular reactors, in order to promote velocity profiles that approach the plug-flow.

CONCLUSIONS

In this paper the modeling of a tubular reactor for MMA polymerization was performed, considering laminar flow conditions. The influence of the main operating parameters (initiator and solvent concentration, heat transfer area) on the reactor behavior was studied.

Small diameter reactors (large specific heat-transfer areas) are more efficient from the point of view of heat transfer, the radial temperature variations are smaller and a product with more homogenous molecular weight is obtained. However, the main drawback of a small diameter is the large pressure drop induced by high flow velocity.

The results illustrate that laminar flow gives an inefficient utilization of the reaction volume, particularly at small solvent to monomer ratios. Due to low velocities near the wall, the polymer accumulates in this region and the heat transfer becomes less efficient.

These inconveniences could be removed by a reactor with a relatively large diameter but equipped with static mixers which homogenize the reaction mixture and improve the radial heat transfer through the polymer layer.

The trends of the main changes induced by the use of static mixers were evidenced by a comparative simulation of the same process in a plug flow tubular reactor. A polymer with higher molecular weight and smaller polydispersion index was predicted in the plug-flow reactor simulation, practically at the same final monomer conversion.

Symbols used

c_M	[mole/L]	monomer concentration
c_I	[mole/L]	initiator concentration
c_S	[mole/L]	solvent concentration
d_t	[m]	reactor diameter
D, D_{ef}	[m^2/s]	mass diffusion coefficients
f	[-]	initiator efficiency
Gz	[-]	Graetz number
k	[$W \cdot m^{-1} \cdot K^{-1}$]	thermal conductivity
k_d	[s^{-1}]	initiation rate constant
k_p, $k_{p,0}$	[$L \cdot mole^{-1} \cdot s^{-1}$]	chain propagation rate constant
k_t ,$k_{t,0}$, $k_{tc,}$ k_{td}	[$L \cdot mole^{-1} \cdot s^{-1}$]	termination rate constant (global, by combination and by disproportionation, respectively)
k_{tm}	[$L \cdot mole^{-1} \cdot s^{-1}$]	chain transfer to monomer rate constant
k_{ts}	[$L \cdot mole^{-1} \cdot s^{-1}$]	chain transfer to solvent rate constant
M_n	[kg/kmole]	number-average molecular weight

Nu	[-]	Nusselt number
r	[m]	radial coordinate
T, T_f, T_b	[K]	reaction, feed and jacket temperature
u_z	[m·s^{-1}]	axial velocity
z	[m]	axial coordinate

Greek symbols

α	[W·m^{-2}·K^{-1}]	partial heat transfer coefficient
ΔH_p	[J·mol^{-1}]	polymerization enthalpy
η	[Pa·s^{-1}]	reaction mixture viscosity
λ_m	[-]	mth order moments for free-radicals concentrations distribution (m = 0, 1, 2)
μ_m	[-]	mth order moments for polymer concentrations distribution (m = 0, 1, 2)
φ_m, φ_p	[-]	monomer and polymer volumetric fractions

REFERENCES

1. S. R. Ponnuswamy, "On-line measurements and control of a batch polymerization reactor", University of Alberta, Edmonton, **1984**, 252.
2. P. E. Baillagou, D. S. Soong, *Polymer Engineering & Science*, **1985**, *25(4)*, 212.
3. A. D. Schmidt, A.H. Ray, *Chemical Engineering Science*, **1981**, *36*, 1401.
4. S.-M. Ahn, S.-P. Chang, H.-K. Rhee, *Journal of Applied Polymer Science* **1998**, *69*, 59.
5. W. Y. Chiu, G. M. Carrat, D.S. Soong, *Macromolecules*, **1983**, *16*, 348.
6. B. M. Louie, D. S. Soong, *Journal of Applied Polymer Science*, **1985**, *30*, 3707.
7. P. E. Baillagou, D. S. Soong, *Chemical Engineering Science*, **1985**, *40(1)*, 75.
8. T. J. Crowley, K. Y. Choi, *Ind. Eng. Chem. Res.*, **1997**, *36*, 3676.
9. A. Husain, A. E. Hamielec, *AiChE Symposium Series*, **1976**.
10. J. S. Vrentas, C. H. Chu, *Chemical Engineering Science*, **1987**, *42(5)*, 1256.
11. J. S. Vrentas, W. J. Huang, *Chemical Engineering Science*, **1986**, *41(8)*, 2041.
12. R. Cintron-Cordero, R. A. Mostello, J. A. Biesenberger, *Can. J. Chem. Eng*, **1968**, 46.
13. S. Lynn, J. E. Huff, *AIChE Journal*, 1971, *17(2)*, 475.
14. C. E. Wyman, L. F. Carter, *AiChE Symposium Series*, **1976**.
15. J. W. Hamer, W. H. Ray, *Chemical Engineering Science*, **1986**, *41(12)*, 3083.
16. I.Banu, G. Bozga, I. Nagy, J. P. Puaux, *Chemical Engineering and Technology*, **2008**, *31(10)*, 1516.

17. P. E. Baillagou, D. S. Soong, *Chemical Engineering Science* **1985**, *40(1)*, 87.
18. R. H. Perry, D. W. Green, J. O. Maloney, "Perry's Chemical Engineer's Handbook", McGraw Hill, New York.**1997**, chapter 5.
19. J. Brandrup, E. H. Immergut, E.A. Grulke, "Polymer Handbook" John Wiley and Sons, Inc., New York, **1999**, section II.
20. B. E. Nauman, "Chemical Reactor Design, Optimization, and Scale up", McGraw-Hill, **2002**, chapter 8.
21. The MathWorks, I., *MATLAB Documentation*, **1984-2008**.